Quaternary Science Reviews 294 (2022) 107739

Contents lists available at ScienceDirect

Quaternary Science Reviews

journal homepage: www.elsevier.com/locate/quascirev

An astronomical age-depth model and reconstruction of moisture availability in the sediments of Lake Chalco, central Mexico, using borehole logging data

Mehrdad Sardar Abadi*, Christian Zeeden, Arne Ulfers, Thomas Wonik

LIAG, Leibniz Institute for Applied Geophysics, Stilleweg 2, 30655, Hannover, Germany

ARTICLE INFO

Article history:
Received 31 March 2022
Received in revised form
29 August 2022
Accepted 29 August 2022
Available online 9 September 2022

Handling editor: P Rioual

Keywords:
Quaternary
Paleoclimatology
Tropical north America
Spectral gamma ray
Authigenic uranium
Magnetic susceptibility
Milankovitch cycles
Cyclostratigraphy

ABSTRACT

Understanding the moisture history of low latitudes from the most recent glacial period of the latest Pleistocene to post-glacial warmth in continental tropical regions is hampered by the lack of continuous time series. We conducted downhole spectral gamma (γ) ray and magnetic susceptibility logs over 300 m of lacustrine deposits of Lake Chalco (Mexico City) to reconstruct an age-depth model using an astronomical and correlative approach, and to reconstruct long-term moisture availability. Our results suggest that the Lake Chalco sediments contain several rhythmic alternations with a quasi-cyclic pattern comparable to the Pleistocene benthic stack. This allows us to calculate a time span of about 500,000 years for this sediment deposition. We developed proxies for moisture, detrital input, and salinity, all based on the physical properties of γ-ray spectroscopy and magnetic susceptibility. Our results indicate that Lake Chalco formed during Marine Isotope Stage 13 (MIS13) and the lake level gradually increased over time until the interglacial MIS9. Moisture content is generally higher during interglacials than during glacials. However, two periods, namely MIS6 and MIS4, have higher moisture contents. We developed a model by comparing the obtained moisture proxy with climatic drivers, to understand how different climate systems drove effective moisture availability in the Chalco sub-basin over the past 500,000 years. Carbon dioxide, eccentricity, and precession are all key drivers of the moisture content of Lake Chalco over the past 500,000 years.

1. Introduction

Quaternary paleoclimate studies have revealed the sensitivity of global temperature fluctuations to abrupt climate transitions (Snyder, 2016; Willeit et al., 2019). Many abrupt climate transitions have occurred on short time scales of centuries or even decades at intervals throughout the Quaternary (e.g., Chalk et al., 2017; Dräger et al., 2019). Knowledge on rapid progressive climate transitions improve predictions regarding the sensitivity of life to current human-induced climate change (Welti et al., 2020). The influence of convection systems in the tropics has recently been shown to have an important role in supplying humidity to the upper troposphere, affecting both higher latitude atmospheric circulation and climate change (Peterson et al., 2000; Metcalfe and Nash, 2012). Despite the known effects of tropics on global climate forcing, the response of tropical regions to climate shifts remains poorly understood (Brown et al., 2019). Quaternary terrestrial stratigraphic records in tropical regions such as long-lived lakes provide valuable information to explore sensitivity to climate change (e.g., Toole, 2019; Ortega-Guerrero et al., 2020). Climate is a major driver of lake water level. In turn, lake water level has strong control over lake physical (e.g. lake stratification), ecological, and biogeochemical processes. For instance, rising lake levels in a drainage basin with positive water balance leads to less water circulation, stratification, and high oxygen depletion rates in bottom waters. Development of anoxic bottom water can enhance the concentration of authigenic uranium in sediments and the preservation of organic matter in the absence of oxidation processes (e.g., Och et al., 2016).

The specific geomorphology of central Mexico, as a result of the system's geological background of subduction zone, has allowed the formation of several extensive lake systems starting at around one million years (Ma) (Ferrari et al., 2012; Arce et al., 2013). The Basin of Mexico (Valley of Mexico), located at the east-central part

* Corresponding author.
E-mail address: Mehrdad.SardarAbadi@leibniz-liag.de (M. Sardar Abadi).

https://doi.org/10.1016/j.quascirev.2022.107739

of the Trans Mexican Volcanic Belt (TMVB), contained five lakes: Chalco and Xochimilco in the south, Texcoco in the center, and Xaltocan and Zumpango in the north. These lakes covered c. 1500 km^2 of the valley floor at 2240 m above sea level (Fig. 1a, Brown et al., 2019; Mazari-Hiriart et al., 2019). The Basin of Mexico is located south of the tropic of cancer and has small seasonal changes in temperature, varying primarily as a function of latitude and elevation. The mild climate and fertile soil made the Basin of Mexico suitable for agricultural activities (Kirkwood, 2010). The area has been continuously populated by humans since colonization of primary civilizations and remains an area with one of the highest population concentrations in the world (Hamnett, 2006).

Human civilization in central Mexico has a long history, and one shaped by temporal changes in climate. The seasonal variability of the low-pressure Intertropical Convergence Zone (ITCZ) is one of main factors controlling the effective moisture pattern over central Mexico, leading to a summer monsoon and dry winter season (Amador et al., 2006). The combination of rapid population growth, anticipated future increases in air temperature and likelihood of droughts in central Mexico, suggests that this will remain a region strongly impacted by changing climate. To understand the potential effects of climate change on Earth's future in a specific region, one key strategy is to study the responses of that specific geographic point – variation in temperature and moisture – to climate changes in the past.

Paleoclimate studies are required to understand what central Mexico, which has been inhabited by dense human civilization for such a long period, was like during the Quaternary (Metcalfe et al., 2000; Lozano-García et al., 2015; Caballero et al., 2019; Ortega-Guerrero et al., 2020). Previous work has examined a part of Lake Chalco's sediments using mineral magnetism, diatoms, and elemental chemistry to highlight the role of insolation in climatic variation. However, previous researchers lacked access to the complete lacustrine sequence of Lake Chalco, presenting a limitation in unravelling the paleoclimate signal through central Mexico. The MexiDrill Project of the International Continental Scientific Drilling Program (ICDP) began in 2016. This project recovered the complete lacustrine sequence of Lake Chalco in order to unravel the climate and ecosystem evolution on millennial to Milankovitch timescales in central Mexico (Brown et al., 2019). Three long drill cores (1 A, 1 B, 1C) were retrieved, recovering ~300 m long lacustrine sequence with 88%–92% recovery. Additionally, cores were recovered into the volcanic basement, down to a total depth of 522 m (details are discussed in Brown et al., 2019). The primary results from ongoing research of the MexiDrill campaign described the sedimentology and stratigraphy of the Lake Chalco as well as the early evolution of the lacustrine environment (Martínez-Abarca et al., 2021; Valero-Garcés et al., 2021). In addition to the core discovery, the Leibniz Institute for Applied Geophysics conducted downhole logging measurements including spectral gamma (γ) ray (SGR) in the 1 A borehole (Fig. 1b, Supplement Material 01). SGR logging depth is considered a true depth and a better representation of length of the complete lacustrine sediments in comparison to the core measurements. SGR is the only tool that can run through a cased hole and as a result, provides a continuous signal of γ-ray and distribution of K, Th and U.

SGR data in boreholes reflect the presence of naturally occurring radioactive elements including potassium (^{40}K), the equilibrium decay series of uranium (^{238}U and ^{235}U and their daughters), and thorium (^{232}Th and daughters). Natural sources of γ radiation in lacustrine deposits can be derived from volcanic ash deposition in the form of tephra or as detrital inputs from eroded sediments containing radioactive elements. Tephra layers contain varying amounts of potassium-rich minerals (K), as well as minerals containing elements of the uranium (U) and thorium (Th) series. The deposition of tephra layers across the lake sediments are unrelated to climate, and create challenges in paleoclimate time series. Natural emanation of γ-ray by sediments, because of the presence of radioactive elements, can reflect the rate of detrital input. We expect that mineral concentrations of K, Th, and U as a result of erosion rate should have a normal distribution with higher values indicating higher detrital input. However, redox conditions in lake water can reduce the mobility of soluble U through conversion to more stable reduced phases (Timofeev et al., 2018) in bottom lake sediments, resulting in higher γ-ray emission. Conversely, extreme dry conditions could lead to the deposition of evaporate minerals containing high amounts of K and Th minerals, resulting in higher γ radiation. SGR data is sensitive to changes in environmental systems and climate, and thus has the potential to reveal past conditions. However, a cyclostratigraphy approach has rarely been applied to downhole logging/γ-ray data (but see Baumgarten and Wonik, 2015; Li et al., 2019; Read et al., 2020; Ulfers et al., 2021; and references therein).

Here we aim to develop the first astronomical age-depth model of the complete lacustrine sequence of Lake Chalco using SGR borehole logging data and a cyclostratigraphic approach. Our second objective is to reconstruct the effective moisture availability by calculating the probability of authigenic U distributed across the lake sediments. We expect that an elevated U content in proportion to the content of K and Th indicate redox conditions in lake bottom water as a result of rising lake level and authigenic mineral formation. K and Th content can be interpreted as a proxy for the rate of detrital input to the lake system. Developing an age-depth model for Lake Chalco allows us to evaluate use of γ-ray proxies for both moisture availability and detrital input with respect to glacial-interglacial variability and precession-derived insolation in central Mexico.

2. Geological background

A convergent boundary of tectonic plates lies below Mexico where the Cocos tectonic plate is subducting beneath the continental edge of the North American plate since the Miocene (~16 Ma, Ferrari et al., 2012). In result of the subduction, a chain of volcanoes, the TMVB, formed in south-central Mexico. The emergence of a long series of volcanic arcs on the continental crust led to the development of an extensive interior drainage basin nearly one million years ago (Arce et al., 2013). In present day, this geological formation is called the Basin of Mexico (Fig. 1a). Since its formation, the water retained in this basin resulted in the formation of several lakes. During periods of high-water levels, this system consisted of one main extensive lake. Before the arrival of the Spanish, Basin of Mexico was occupied by the Aztec people who built a large city called Tenochtitlan on and around the lake system. In the early 1600s CE, the Spanish drained most of the lake system in an attempt to control flooding. Present day Lake Chalco is a relict water body to the south of present day Mexico City, in the location formerly covered by the larger lake system (Ortega-Guerrero et al., 2017).

2.1. Sedimentology

Sedimentological observations in the 1 A borehole at ~300 m depth confirms the establishment of an initial lake system in the Basin of Mexico after a period of alluvial to fluvial deltaic phases (Martínez-Abarca et al., 2021). Five main lithotypes were identified in lacustrine deposits of Lake Chalco including clastic, carbonate, organic rich sediments, diatomaceous and volcanoclastic material (Ortega-Guerrero et al., 2017; Valero-Garcés et al., 2021). The clastic facies consist of faintly laminated silt with a variable content of

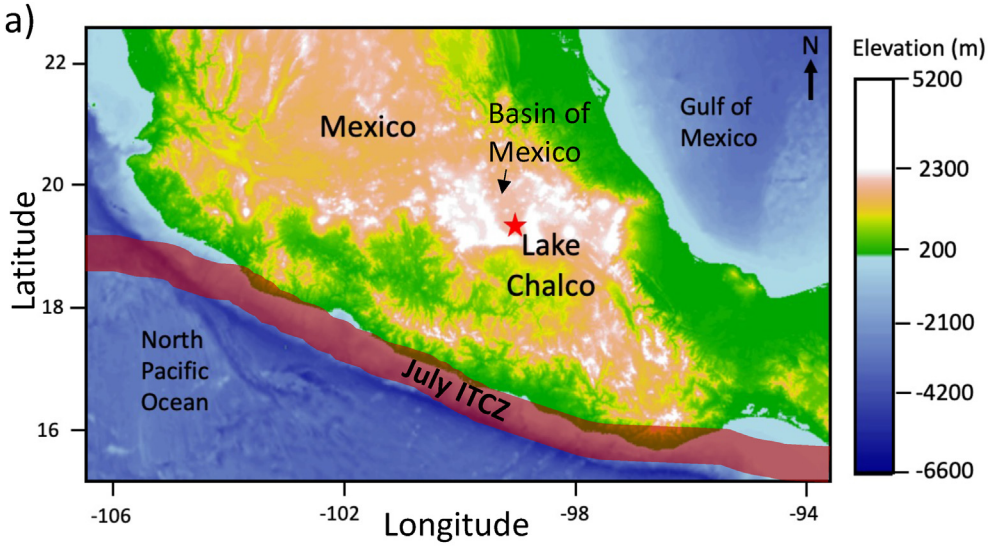
a)
Mexico
Basin of Mexico
Gulf of Mexico
Lake Chalco
North Pacific Ocean
July ITCZ
N
Elevation (m)
5200
2300
200
-2100
-4200
-6600
Latitude
22
20
18
16
-106
-102
-98
-94
Longitude

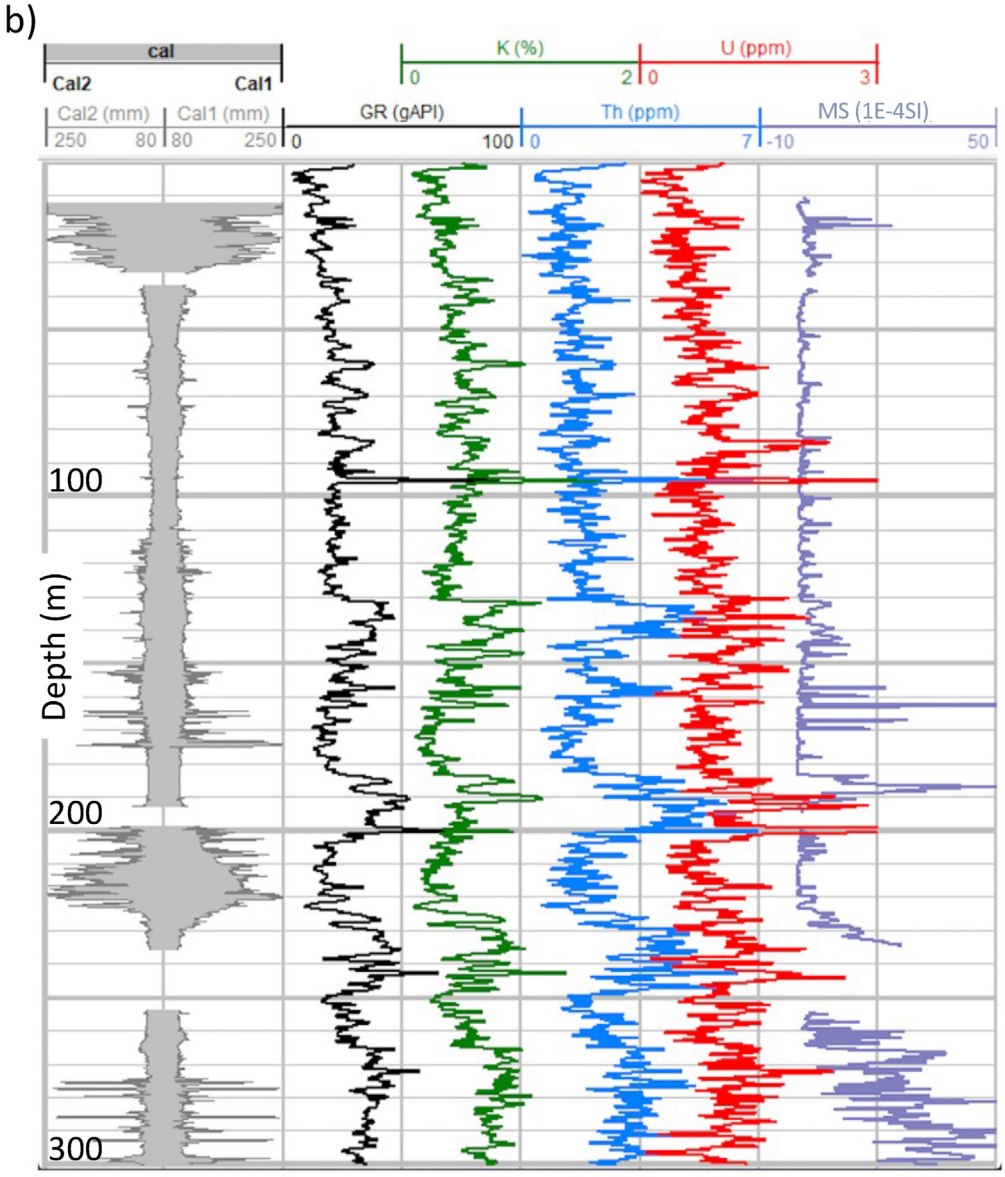
b)
cal
Cal2
Cal1
K (%)
U (ppm)
Cal2 (mm)
Cal1 (mm)
GR (gAPI)
Th (ppm)
MS (1E-4SI)
250
80
80
250
0
100
0
2
0
3
0
7
-10
50
100
200
300
Depth (m)

sand and clay fractions, reflecting distal deep lake environments with low productivity. Laminated diatomaceous sediments are associated with organic rich sediments, and represent deposition during periods in time and space when the lake was deep and productive. Sediments containing saline diatom assemblages associated with carbonate reflect deposition in shallower phases (Valero-Garcés et al., 2021). Volcanoclastic sediments include fragmental material that was produced either by volcanic eruption such as tephra or reworked and redeposited by fluvial currents (Ortega-Guerrero et al., 2017).

2.2. Stratigraphy

Establishing a chronostratigraphic framework for the lacustrine deposits of Lake Chalco is challenging. Challenges include a limited number of radiometric techniques to date sediments, different uncertainty ranges for different techniques, and correlating horizons across multiple boreholes to develop an accurate chronological framework. Currently, several methods have been used to date sections of Lake Chalco. Radiometric methods used for dating the lacustrine sediments in Lake Chalco include Radiocarbon dating (^{14}C) and Uranium—Thorium dating ($^{234}U/^{230}Th$). Carbon dating of pollen and ostracods extracted from five sediment samples from the CHA08 core at Lake Chalco (0.5 km south of current study MexiDrill site) resulted in a ~40 ka (kilo years) age for the upper 36 m of sediments (Herrera-Hernández, 2011; Ortega-Guerrero et al., 2017). $^{234}U/^{230}Th$ dating carried out on extracted zircons from a tephra layer suggest a 76.7 ka age at the depth of 63 m in CHA08 core (Ortega-Guerrero et al., 2017). The transition between MIS 5 and MIS 6 was identified at the depth of 106 m based on the diatom analyses (Martínez-Abarca et al., 2021). The MIS 6 − MIS 5 transition is assigned an age of 130 ± 3 according to the Lisiecki and Raymo (2005) chronology. Four samples were taken from a carbonate rich horizon at the depth of 195 m of the MexiDrill site. Two of them have been dated at 231 ± 11 ka and 332 ± 14 ka, and two others returned infinite dates using a$^{234}U/^{230}Th$ dating technique (Martínez-Abarca et al., 2021). Combining all these dating sources, Martínez-Abarca et al. (2021) developed a Bayesian age-depth model based on the available radiometric data and using sand and volcanoclastic sediments as instantaneous deposited material to correlate the cores. The Bayesian age-depth model developed by Martínez-Abarca et al. (2021) has an age of 408 ± 47 for the upper 343 m at the MexiDrill site. However, the age suggested for below 106 m should be used cautiously due to either a lack of dating or a likely inaccurate $^{234}U/^{230}Th$ dating technique used on the carbonate samples at the depth of 195 m.

3. Methods

3.1. Site location

The study area (19°15′N, 98°58′W) is located near the depocenter of Lake Chalco, in the southern part of the Basin of Mexico with a lacustrine plain at 2240 m above sea level (Brown et al., 2019). The targeted site (borehole 1 A: 19°15′ 25.9″N, 98°58′ 31.8″W) was drilled as part of the International Continental Scientific Drilling Program (ICDP) MexiDrill program to a total depth of 522 m with 88% core recovery (Brown et al., 2019).

3.2. Borehole logging

The Leibniz Institute for Applied Geophysics conducted the downhole logging measurements, including spectral γ-ray (SGR) and magnetic susceptibility (MS) measurements. The SGR tool has a 10 cm vertical resolution of measurements and was run at 3 m/min logging speed, while the MS probe has a 2 cm vertical resolution and was run at 3 m/min. The SGR was recorded through the drill string using the SGR70 probe (type 1419), while the MS data was collected using a Micro-Susceptibility tool (type 1121) in the open hole. Both sondes are manufactured by Antares (Germany).

γ-ray spectrometry is an analytical technique that displays γ-ray flux as an energy distribution of emitted photons from source isotopes (Hendriks et al., 2001). The natural γ radiation originated from naturally occurring U, Th and K. A γ -ray spectrum can be broken into constituent energy signals corresponding to specific isotopic signatures. Each γ-ray photon has a discrete energy level indicative of specific source isotopes. The relative count of specific photons emitted from U, Th and K are related to their abundance.

The magnetic susceptibility tool applies an external magnetic field and measures the induced magnetization, which indicates the amount of ferromagnetic minerals in sediments along the borehole depth. The MS data are corrected for the variation in borehole diameter and temperature. We compared the result with the initial 88% recovered core described by Brown et al. (2019). In order to adjust the core depth with the logging depth, we correlated the MS signals of the core and borehole log using the 'linterp' function in the 'astrochron' R package (Meyers, 2014; Supplement Material 02).

3.3. Time series analysis

In order to extract the primary non-volcanic signals caused by climatic agents and corresponding environmental changes, we first detected and removed signals from embedded tephra layers in lacustrine sediments of Lake Chalco (Supplement Material 03) by comparing with representative horizons of tephra from the core analyzed by Brown et al. (2019). We standardized the radiogenic elements and γ-ray time series to be on the same scale. We rescaled the time series to have a mean of zero and a standard deviation of one.

To determine if the γ-ray signal has quasi-regular cyclicity, we tested for the presence of regular cycles using wavelet analysis using the biwavelet R package (Gouhier et al., 2021; R Core Team, 2022, Fig. 2). Wavelet transformation is a hierarchical grading of time and period (or frequency) information to compute which cyclical components at which period turn on or off across time or depth.

Next, we assessed the rate of sedimentation (SR) across the logged interval. SR was calculated using the timeOpt method (Meyers, 2015, 2019) as implemented in the R package astrochron (Meyers, 2014). This method estimates the fit of data and astronomical cycles testing a suite of different SR, and here also SR as function of lithology (timeOptTemplate) assuming high sedimentation during high SGR coinciding with high SR. The timeOpt method uses information of both a power spectrum, precession amplitude, and its fit with reconstructed eccentricity for a given SR, and tests this for a suite of SR (Fig. 3). Using timeOpt, we calculated both a linear increasing in SR using an optimized r^2 model and estimates of SR changes with lithology (here as SGR) with depth

Fig. 1. a) Map of central Mexico. An asterisk marks the location of Lake Chalco in the Basin of Mexico. The tropical rain belt known as Intertropical Convergence Zone (ITCZ) moves northward from the Equator during the northern hemisphere summer (e.g., Ortega-Guerrero et al., 2020). b) Borehole logging data of Lake Chalco including caliper (in millimeters), spectral γ-ray along with radiogenic elements (K, Th, and U), and magnetic susceptibility (MS). Caliper log measures the diameter of the borehole along its depth, and indicates the existence of caves and shale swelling in the borehole. γ-ray spectrometry measures γ-ray energy distributed from the sediment in respect to the source isotopes (K, Th, and U). The magnetic susceptibility log indicates the amount of ferromagnetic minerals in sediments along the borehole depth.

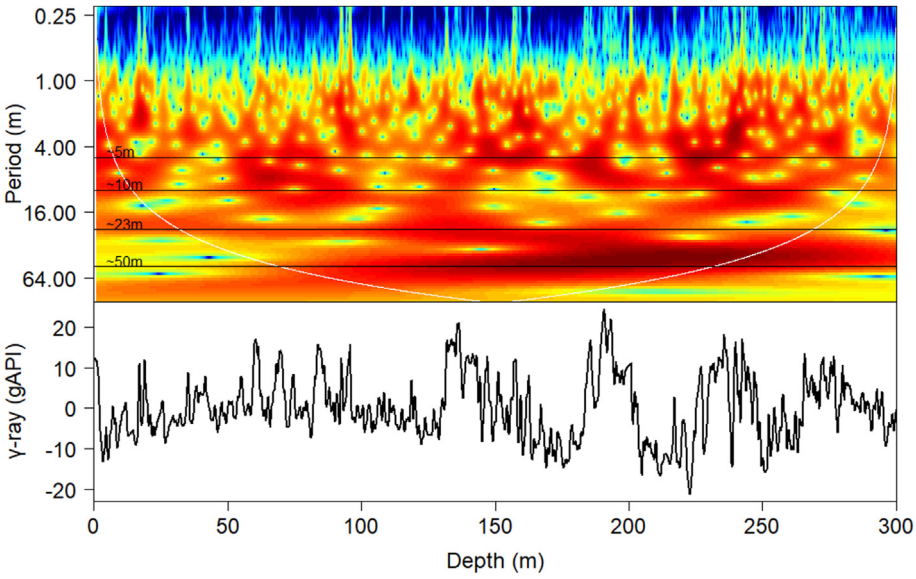

Fig. 2. Wavelet analysis (top) of the detrended γ-ray signal (bottom) recorded across the lacustrine deposits of Lake Chalco. The color code in the wavelet analysis indicates high cyclicity (red) and low cyclicity (blue) for depth (abscissa) and different periodicity (ordinate). White shading highlights parts not fully covered by data. (For interpretation of the references to color in this figure legend, the reader is referred to the Web version of this article.)

(Meyers, 2015, 2019). To scale our timeOpt model for instantaneous accumulation optimization, we use the 'template' argument in the astrochron R package (Meyers, 2014). We then applied the estimated SR from the assessment using SGR as proxy for SR to determine the age across the log. We further improved the age model by comparing and correlating the time series with a record of benthic $\delta^{18}O$ representing global climate evolution (LR04 stack, Lisiecki and Raymo, 2005). In order to tune the γ-ray time series of Lake Chalco with the LR04 stack, we selected several tie points that are coinciding to beginning and end of the Marine Interglacial Stages (MIS). Tie points represent the smallest scale used for correlating the γ-ray series of Lake Chalco with the LR04 stack. Although we are sure of the exact position of tie points on the reference age model (LR04), the corresponding depth of points in the γ-ray time series are not certain and require uncertainty estimation. For instance, the end of the MIS7 has been considered as a strong tie point proxy for correlation among the climate/ice sheet models (Fig. 4). Tie points are available in the Supplement Material 04. Filtering of the dataset was done using a Taner filter (Taner, 1992; Zeeden et al., 2015), and using the 'astrochron' R package (Meyers, 2014). Lastly, we compare the available published radioisotope dating with astronomical ages (Herrera-Hernández, 2011; Ortega-Guerrero et al., 2017; Martínez-Abarca et al., 2021) to evaluate the accuracy of the tuned astronomical timeframe (Fig. 5).

3.4. Spectral γ-ray proxies

To unravel the paleoclimate and paleoenvironmental conditions using our γ-ray borehole logging data, we make several assumptions in our calculations of climate proxies. We assume that there are four sources of the γ-ray emission across lacustrine deposits of Lake Chalco: detrital silicate minerals produced by physical and chemical weathering, volcanic ash deposited as tephra layers, authigenic uranium associated with reducing conditions at the lake bottom and in lake bottom sediments, and deposition of evaporite minerals. To evaluate our proxies, we compare our SGR proxies with available paleontological proxies on Lake Chalco (Ortega-Guerrero et al., 2020). Ortega-Guerrero et al. (2020) presented the relative abundance of diatom ecological groups and selected species that are commonly considered as a proxy for lake salinity and depth. Ortega-Guerrero et al. (2020) defined ecological diatom groups that characterize nearly opposite lake conditions and used these as a proxy to track changes from deep to shallow lake levels. The relative abundance of *Stephanodiscus* spp., and small Fragilariaceae species are evidence for a freshwater and deeper lake, whereas the sum of alkaliphilous and halophilous taxa are indicative of higher salinity and shallower conditions (Fig. 6). The diatom species distribution covers a period of 115 kyr (late MIS6 to MIS3) across the lacustrine deposits of Lake Chalco (Ortega-Guerrero et al., 2020, Fig. 6).

The distribution of freshwater diatom taxa and the sum of the taxa indicative of higher salinity and shallower conditions were used to examine the accuracy of our proposed salinity and moisture proxies respectively (the mentioned proxies are discussed at 3.4.2 and 3.4.3 sections, Fig. 7).

3.5. Detrital proxy

Cations (e.g., Mg, Na, K) in the crystal lattice of plagioclase minerals increase the minerals' susceptibility to weathering reactions. Chemical weathering depends on climate and is particularly enhanced by the amount of precipitation in tropical regions with high temperatures such as central Mexico. Geochemical analyses of the TMVB in south-central Mexico suggest a basaltic to dacitic composition (65–70% SiO_2, 2–6% $Na_2O + K_2O$, Arce et al., 2019). Potassium-40 (^{40}K) and the equilibrium decay series of thorium (^{232}Th and daughters) and uranium (^{238}U and ^{235}U and their daughters), are the three main elements which emanate natural γ-ray radiation. The concentration of K and Th in lacustrine sediments are indicative of igneous rocks. U preserved in sediments can represent two input sources: detrital U derived by erosion of volcanic rocks and authigenic U from redox-driven precipitation of U out of solution.

Therefore, natural emanation of γ-ray by sediments from the presence of ^{40}K and Th potentially reflects the rate of detrital input. The magnetic susceptibility record of the Lake Chalco sediments (Fig. 1b) has been linked to the detrital flux originated from the surrounding hinterland (Ortega-Guerrero et al., 2020). We expect

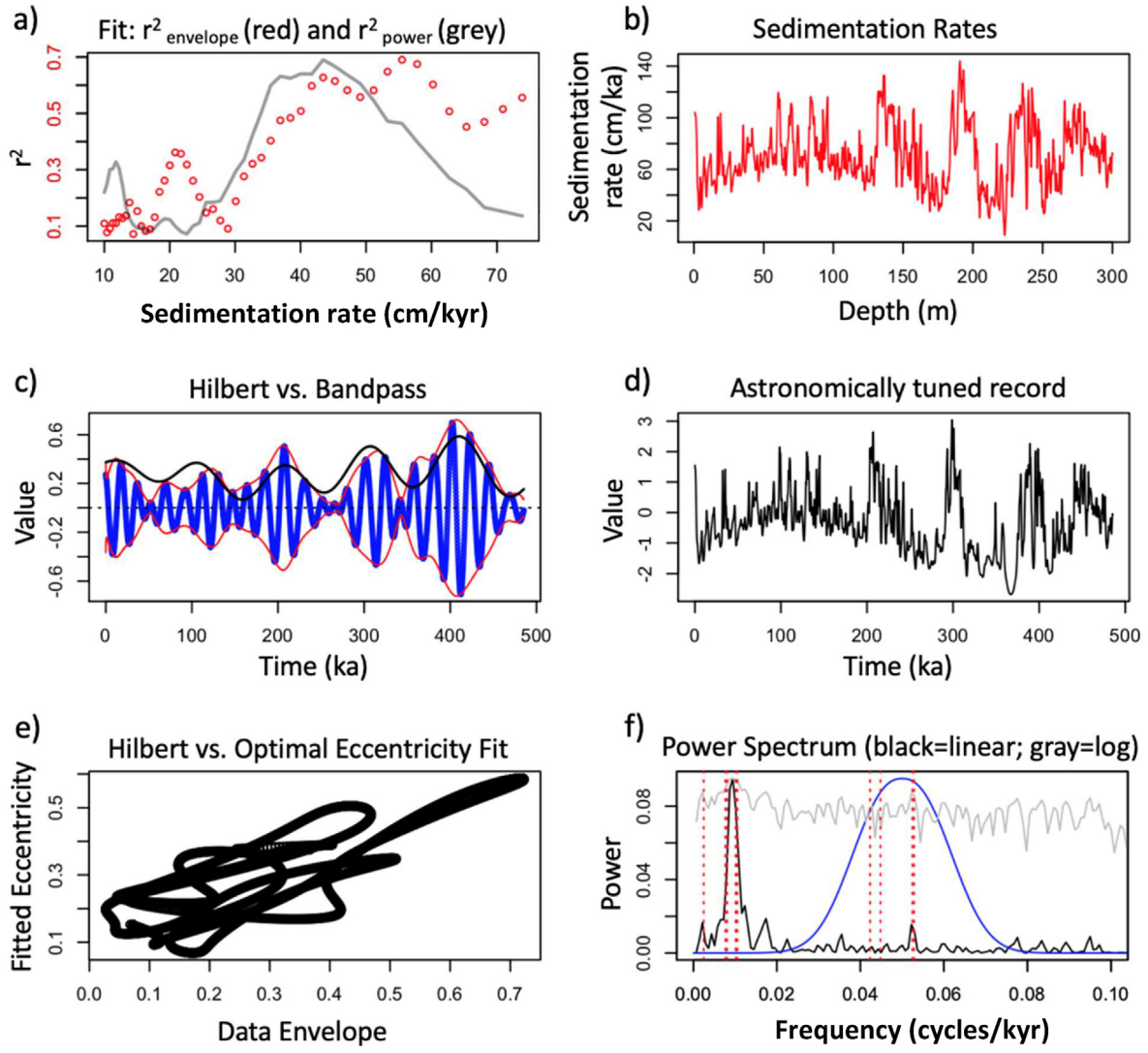

Fig. 3. TimeOpt template analysis on the detrended spectral γ-ray signal (SGR) for the upper 300 m of Lake Chalco. a) Squared Pearson correlation coefficient for the amplitude envelop fit (r^2 envelop, red dots) and the spectral power fit (r^2 spectral, gray line) at each evaluated sedimentation rate. b) timeOpt-reconstructed sedimentation rate history. c) Comparison of the band-passed precession signal (blue line), the data amplitude envelope (red line), and the timeOpt-reconstructed eccentricity model (black line). d) Astronomically-tuned stratigraphic series using the sedimentation rate history in (b). e) Crossplot of the timeOpt-reconstructed precession amplitude and the eccentricity models. f) Power spectrum of the Multitaper method (MTM) for the timeOpt derived age model and GR data using the average sedimentation rate of 43.5 cm/kyr. Black line: linear spectrum; gray line: log spectrum. The blue line indicates the bandpass filter for evaluation of the precession amplitude envelope. Vertical dashed red lines indicate the eccentricity and precession target periods. (For interpretation of the references to color in this figure legend, the reader is referred to the Web version of this article.)

that mineral concentrations of K and Th as result of weathering and erosion should positively covary with the MS signal, as both are indicative of detrital input. In the case of Lake Chalco, the K–Th signal driven from SGR borehole are significantly correlated with MS indicating the detrital origin of K and Th contents in lacustrine sediments ($R^2 = 0.29$; Supplement Material 05). We calculated the detrital proxy by summing sediment K and Th content. To better identify the signal of the underlying causal processes, the detrital proxy is smoothed using a 1-m moving average (Fig. 8e). We apply power spectrum on the detrital proxy to describe the amplitude fluctuation present at different oscillation frequencies using the Multitaper method (MTM) spectral analysis (Thomson, 1982; Meyers, 2014).

3.6. Salinity proxy

Increased salinity across the lacustrine deposits of the Lake Chalco may indicate the development of warm and dry conditions in central Mexico during the Quaternary leading to both more saline and therefore higher evaporation rates and the reduction in riverine inputs. These dry conditions cause lake water to become denser in the concentration of ions such as potassium cations (K^+), and alkali metals tend to bond with a halogen and create ionic salts, particularly potassium chlorides, resulting in higher γ-ray emission. The concept of the salinity proxy is that dry periods should be characterized by higher concentrations of K^+ among the lacustrine deposits in comparison to the values expected from detrital input. A rolling correlation is applied to identify the correlation between K and magnetic susceptibility (itself a proxy for detrital input) across the time series using a 1-m rolling window (value calculated for each 10 measurements). Rolling correlation values range between 1 (maximum correlation coefficient) and −1 (minimum correlation coefficient). Negative correlations indicate excessive K content in comparison to expected detrital input. This is interpreted as an

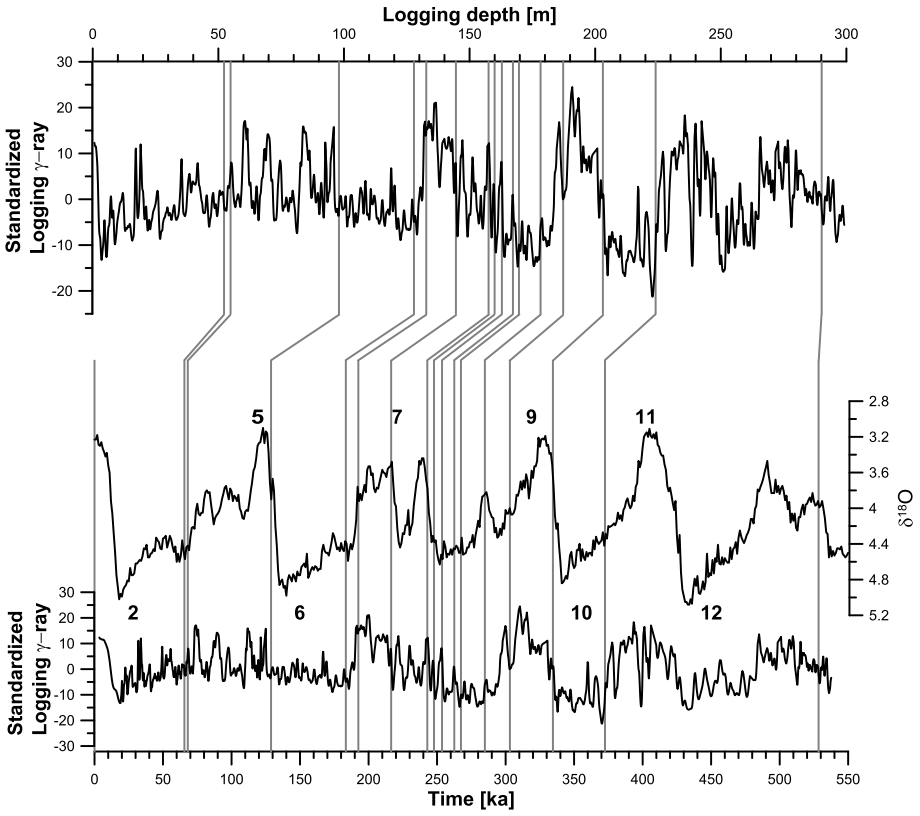

Fig. 4. Correlation of Lake Chalco's Standardized γ-ray depth series to the globally distributed marine benthic oxygen isotope stack ($\delta^{18}O$) and its age model (LR04 stack, Lisiecki and Raymo, 2005), and resulting age-depth model. Vertical gray lines indicate the position of tie points, and numbers point out the marine isotope stages (MIS).

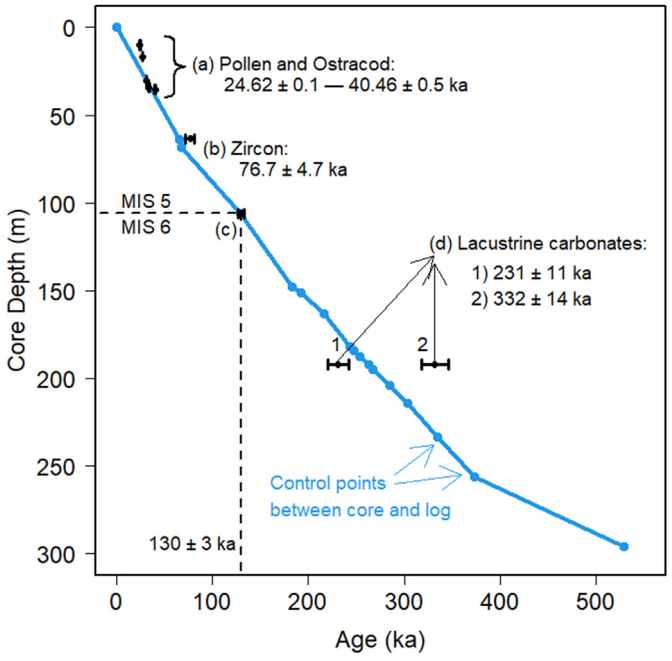

Fig. 5. Age-depth model from our study (blue) and absolute ages of radioisotopes. a) ^{14}C dating of pollen and ostracods (Herrera-Hernández, 2011; Ortega-Guerrero et al., 2017). b) $^{234}U/^{230}Th$ dating of extracted zircons from a tephra layer (Ortega-Guerrero et al., 2017). c) MIS6-5 transition. d) $^{234}U/^{230}Th$ dating of the lacustrine carbonate (Martínez-Abarca et al., 2021). (For interpretation of the references to color in this figure legend, the reader is referred to the Web version of this article.)

increase in the concentration of K because of high-salinity conditions (Fig. 6). A positive correlation between K and magnetic susceptibility indicate the majority of K is of detrital origin. A rolling correlation between K and magnetic susceptibility results in 81% positive values, suggesting a dominantly detrital origin of K among the lacustrine deposits. The average diatom content in shallower lake system (alkaliphilous and halophilous taxa; Ortega-Guerrero et al., 2020) was higher when the salinity proxy was negative (Fig. 7a).

3.7. Moisture proxy

In order to develop a proxy for variation in moisture content across the Lake Chalco sediments, we examined the probability of authigenic uranium concentration. A rolling correlation is applied between U and K−Th (as a detrital proxy) to visualize the variation in the correlation time series over time as a 1-m rolling window. Rolling correlation values range between 1 and -1. Values between 0 and -1 indicate that U content declines with K and Th content. Negative correlations are caused by excessive U content if the U content increases toward the negative values of the correlation (Fig. 6). This is interpreted as precipitated uranium as a result of redox conditions. Samples with negative correlations between U content and K−Th significantly increase with U content within Lake Chalco sediments. Samples with positive correlations between U and K−Th content indicate a detrital origin of U and dominant oxic condition in the lake system. As U content positively varies with K−Th content (decreasing and increasing), we expect that there is no correlation between positive values of the rolling correlation and U content. Given that Lake Chalco is a hydrologically closed basin, development of redox conditions as a result of rising lake

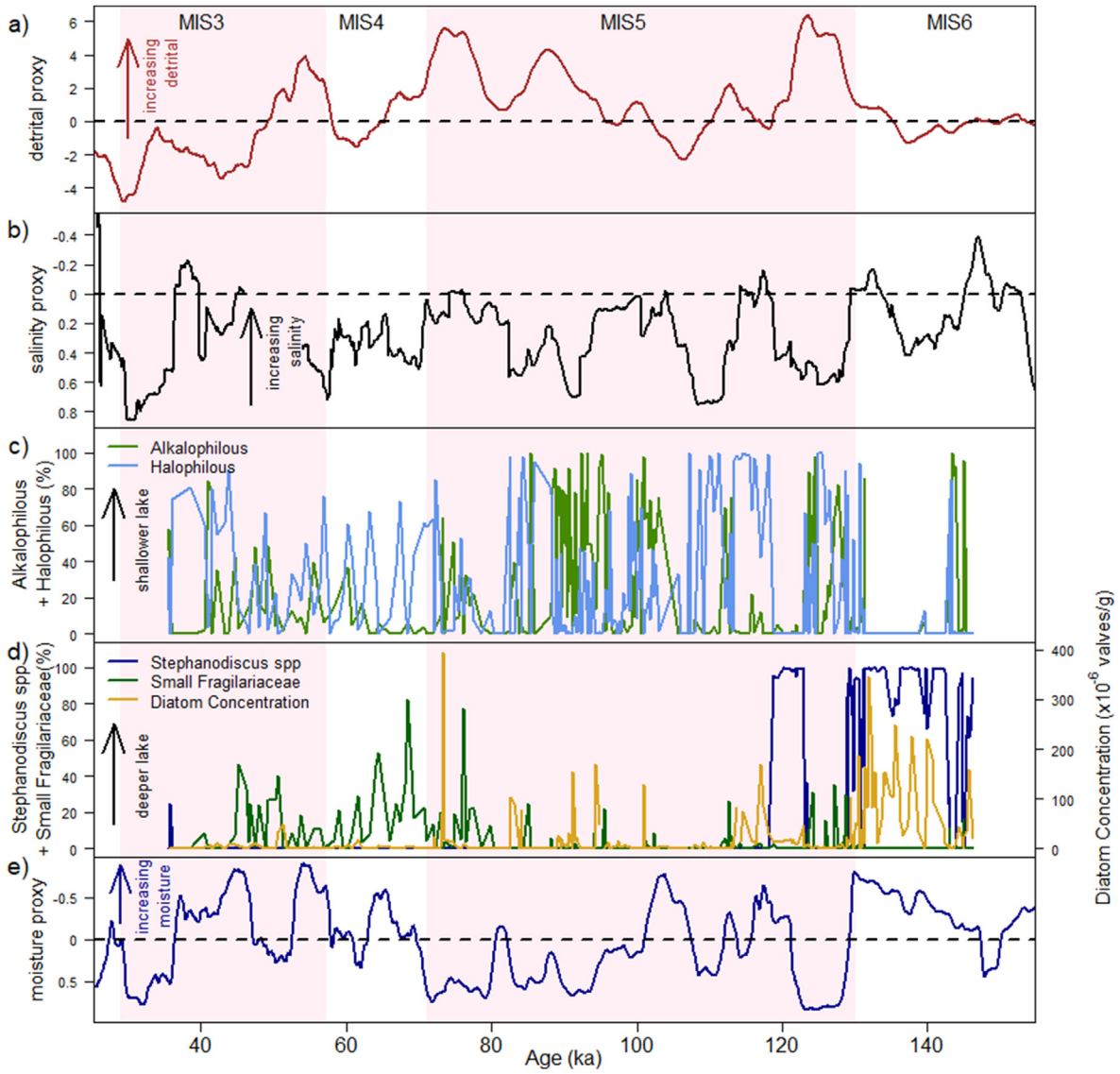

Fig. 6. Comparison of the detrital (a), salinity (b) and moisture (e) proxies with the percentage of diatom species (Ortega-Guerrero et al., 2020) which are indicative for saline and shallower conditions (c) and freshwater and deeper lake (d). Please note that the negative values of salinity and moisture proxy values indicate higher salinity and moisture content as indicated by arrows on the left. MIS stands for marine isotope stages based on the globally distributed marine benthic oxygen isotope (LR04 stack, Lisiecki and Raymo, 2005). MIS with even numbers stands for cold and glacial stages, and odd MIS stands for warm and interglacial stages.

level can be a signature of enhanced moisture availability. To evaluate the moisture proxy, we examined differences in the percent of the diatom species that are indicative of a freshwater and deeper lake (*Stephanodiscus* spp., and small Fragilariaceae species; Ortega-Guerrero et al., 2020) for the negative versus positive values of our moisture proxy (Figs. 6 and 7b). The negative moisture proxy values has significantly larger average percentages of these diatom species.

3.8. Climate drivers

We used linear regression analysis to identify the role of Earth's orbital cycles, carbon dioxide, insolation, and global ice volume as drivers of our moisture proxy. We computed insolation quantities for 20°N latitude (Laskar et al., 2004) across the time period estimated for Lake Chalco's sediments. A record of carbon dioxide concentration from 800 ka until present (Lüthi et al., 2008) and a Pliocene–Pleistocene stack of benthic $\delta^{18}O$ records as a proxy for changes in global ice volume (Lisiecki and Raymo, 2005) were tuned to a similar time scale using the 'linterp' function in the 'astrochron' R package (Meyers, 2014). The full model was specified as:

Moisture proxy ~ eccentricity + obliquity + precession + carbon dioxide + insolation + global ice volume.

High correlation among the predictor variables causes multicollinearity, which eventually reduces the precision of the estimated coefficients and weakens the statistical power of regression models. To identify potential multicollinearity, we calculated variance inflation factor (VIF) between Earth's orbital cycles, insolation, carbon dioxide, and sea surface temperature, and removed variables with a VIF >5 (James et al., 2017). Among the predictor variables, precession and insolation had high variance inflation (VIF >10, $r^2 = 0.96$), thus we removed insolation from the full model prior to model comparison. The resulting model included the moisture proxy as the response variable and driver variables of precession, obliquity, eccentricity, CO_2, and benthic $\delta^{18}O$.

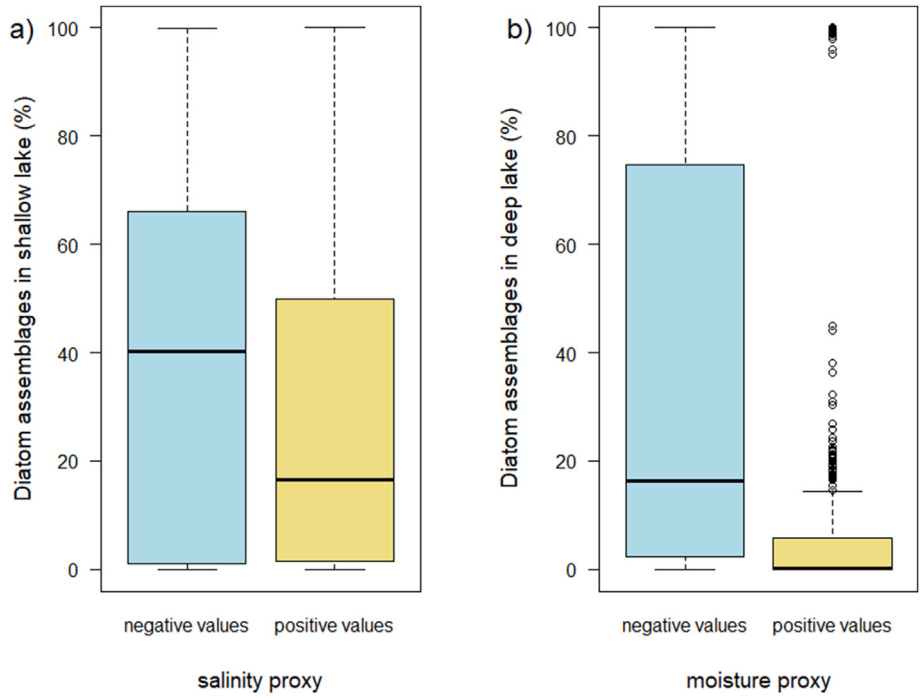

Fig. 7. The distribution of negative and positive values of salinity (a) and moisture (b) proxies illustrated through the average number (abundance) of diatom species indicative of higher salinity and shallower conditions (alkaliphilous and halophilous taxa; Ortega-Guerrero et al., 2020) and indicative of freshwater and deeper lake (*Stephanodiscus* spp., and small Fragilariaceae; Ortega-Guerrero et al., 2020) respectively.

In order to determine potential regulators of moisture, we used an Akaike's Information Criterion corrected for small sample size (AIC_c) framework to identify top models. The AIC framework compares multiple combinations of predictors to determine the best model(s) for a given dataset. The lowest AIC scores indicate the best model fit. We used an additive linear regression model and AIC selection to examine the relative importance of drivers of moisture. The initial model and all reduced additive models were compared using the *dredge* function in the MuMIn R package (Bárton, 2020). The *dredge* function fits every combination of predictors (model driver variables) and weights them by Akaike Information Criterion (AIC). To select the most representative models from the large set of computational models, we examined ΔAIC_c, considering models with a $\Delta AIC_C < 2$ as top models (Burnham and Anderson, 2003).

4. Results

4.1. γ-ray signal

The recorded γ-ray signal across the upper 300 m of the lacustrine deposits of Lake Chalco (Fig. 1b) exhibits strong variation ranging from 4.6 API to 53.5 API. The γ-ray signal has a decreasing trend from the bottom to the top of the log, likely because of compaction increasing with depth. In addition to a previous correction to diminish the effect of volcanic ash deposits through removing the tephra layers, we removed the compaction trend to avoid the effect of compaction on γ-ray frequencies. γ-ray is strongly correlated with the natural radioactive elements including K ($R^2 = 0.71$), Th ($R^2 = 0.69$), and U ($R^2 = 0.54$). Correlations among the three radioactive elements are significant with the tightest relationship between K and Th ($R^2 = 0.40$), and weaker correlations of U with K ($R^2 = 0.18$) and Th ($R^2 = 0.11$, Supplement Material 06). The γ-ray signal is positively correlated with borehole magnetic susceptibility values (MS; $R^2 = 0.26$). The MS signal represents a general record of climate-driven detrital influx (Ortega-Guerrero et al., 2020), but is likely influenced by post-depositional dissolution of iron oxides and the precipitation of iron sulphides at least in layers with high organic matter contents. Covariation between MS and K and Th content exhibits a significant positive correlation ($R^2 = 0.29$), while the correlation between U and MS is positive but weak ($R^2 = 0.04$). γ-ray values follow a unimodal distribution which is positively skewed (right tail, skewness [sk] = 0.30, Supplement Material 07). The individual radiogenic elements follow a similar unimodal pattern although with different skewness as K (sk = 0.20), Th (sk = 0.91), and U (sk = 1.43). The U time series contains a few high values among many low values (log distribution), with large values forcing γ-ray values toward a positive skew. Measurements from which U is correlated positively with K and Th content ($r > 0$) have γ-ray values that exhibit a normal distribution. In contrast, measurements from which U is correlated negatively with K and Th content ($r < 0$) have γ-ray values with a right skewed (Supplement Material 08).

4.2. Astronomical forcing

Existence of regular cyclicity in γ-ray logs is confirmed using wavelet analysis (Fig. 2). The wavelet analysis has reconstructed the depth evolution of the main oscillating components of the γ-ray time series. A cycle with a dominant period around 50 m occurs between 300 m and 100 m depth. A white shading in Fig. 2 highlights the cone of influence, which is not fully covered by data. Another periodic component appears as a horizontal band centered at a period of 23 m. The periodic band at around 23 m evinces a slight increase of period by increasing depth from around 20 m above 10 m–25 m at a depth of 300 m. Within the range of periods of 10 m and 5 m, the wavelet power spectrum reveals several localized components with a discontinuity in the periods. The oscillating components become more discontinuous and less likely to present the cyclic occurrence pattern.

Lacustrine deposits of the Chalco basin preserved cyclic

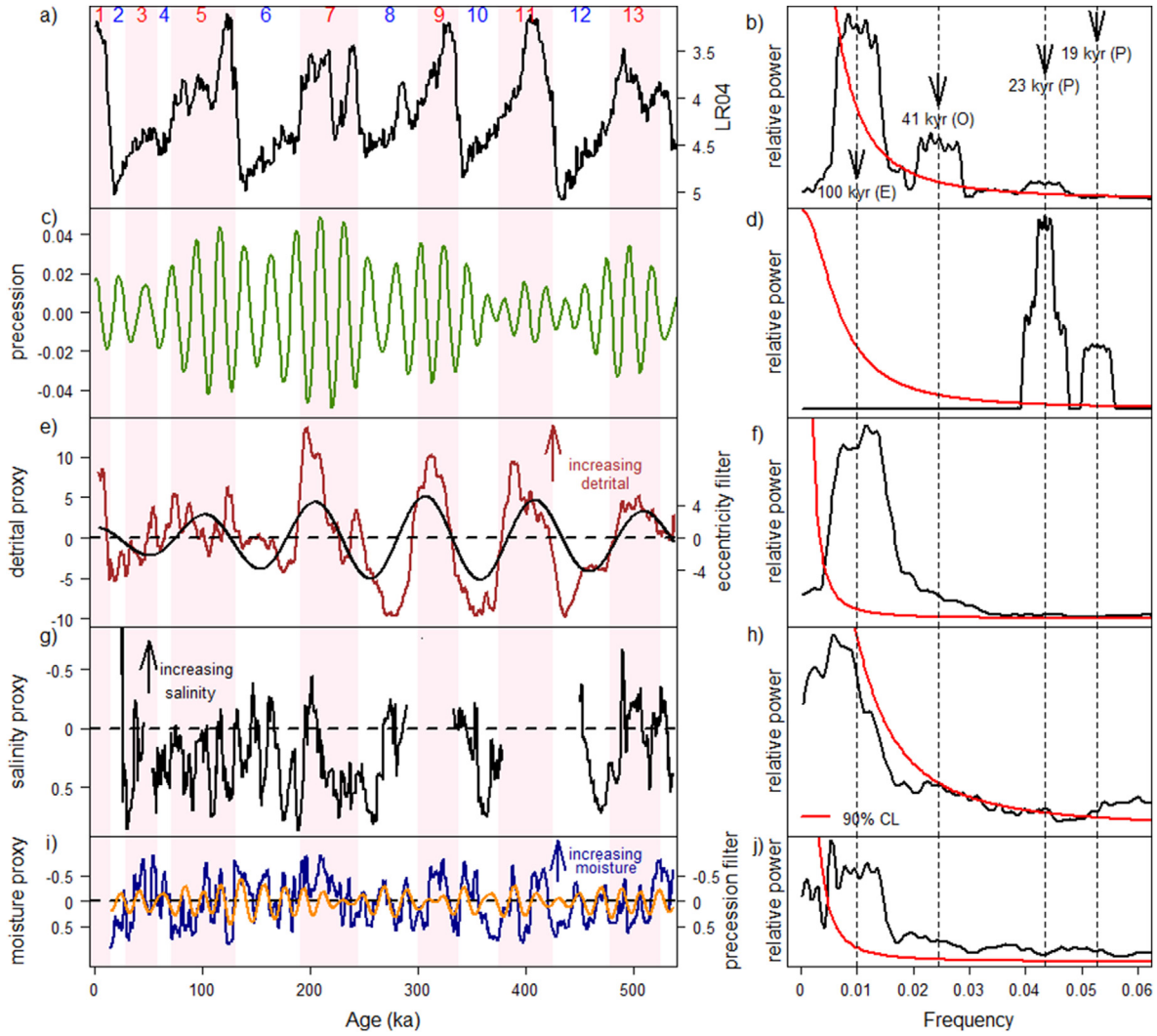

Fig. 8. Comparison of SGR proxies' time series with the globally distributed marine benthic oxygen isotope (a, LR04 stack, Lisiecki and Raymo, 2005), and precession (c). The power spectra of each time series are shown next to the corresponding time series (b, d, f, h, and j). The vertical dashed lines indicate the eccentricity, obliquity, and precession target periods. A 90% confidence level (90% CL) is illustrated to distinguish significant peaks from the spectral background. Taner filters with bandwidth of 125–90 ka and 27–15 ka are applied on detrital (e) and moisture (i) proxies respectively. The salinity proxy (g) is not a continuous record due to the lack of magnetic susceptibility data.

components at different periods as revealed by wavelet analysis. The spectral γ-ray signal provides an ideal case study to use the timeOpt approach for assessing astronomical forcing across the lacustrine deposits, and to create a time scale for the lacustrine sediments (e.g., Ulfers et al., 2022). The initial average SR calculated by timeOpt exceed 43.5 cm/kyr ($r^2 = 0.5$; Fig. 3a and b). We use a template for SR which is driven by the γ-ray proxy (Fig. 3b), which is in agreement with the interpretation of the γ-ray and MS signals implying higher detrital input with higher values. The resulting (tuned) power spectrum for the EP (eccentricity and precession) model displays a strong concentration of ~100 kyr and ~20 kyr cycles (Fig. 3f).

4.3. Age–depth model

We tune the Lake Chalco time series with a stack of globally distributed marine benthic oxygen isotope data (LR04 stack; Lisiecki and Raymo, 2005), based on existing age information (from the estimated 408 ± 45 ka by Martínez-Abarca et al., 2021). The duration of lacustrine deposits extended to over a period of 500 kyr according to our tuned age model (Fig. 4). A test of precession amplitude vs. eccentricity confirms the presence of strong astronomical signals in the Lake Chalco time series (Supplement Material 09). The observed precession modulation of the Lake Chalco's time series is compared with the theoretical eccentricity of the astronomical solution, and precession modulation of the LR04 stack. Eccentricity has a minimum around 400 ka, and while the periodicity is similar, the correlation between the signal amplitudes (400 kyr signal) is poor (Supplement Material 09).

To evaluate our orbitally tuned timeframe, we calibrate the previously available radio-isotopic ages with established astronomically tuned timescale across the lacustrine deposits. We adjusted the core depth with log depth to establish the tuned astronomical age across the core depth (Supplement Material 02). The comparison between our astronomical and correlative period and radio-isotopic ages confirms the consistency of our astronomical tuned time scale (Fig. 5). The result is a robust cyclostratigraphic framework across the Lake Chalco lacustrine deposits.

4.4. Glacial-interglacial variation in SGR proxies (Figs. 8 and 9)

Our moisture proxy is calculated as an index of the likelihood of

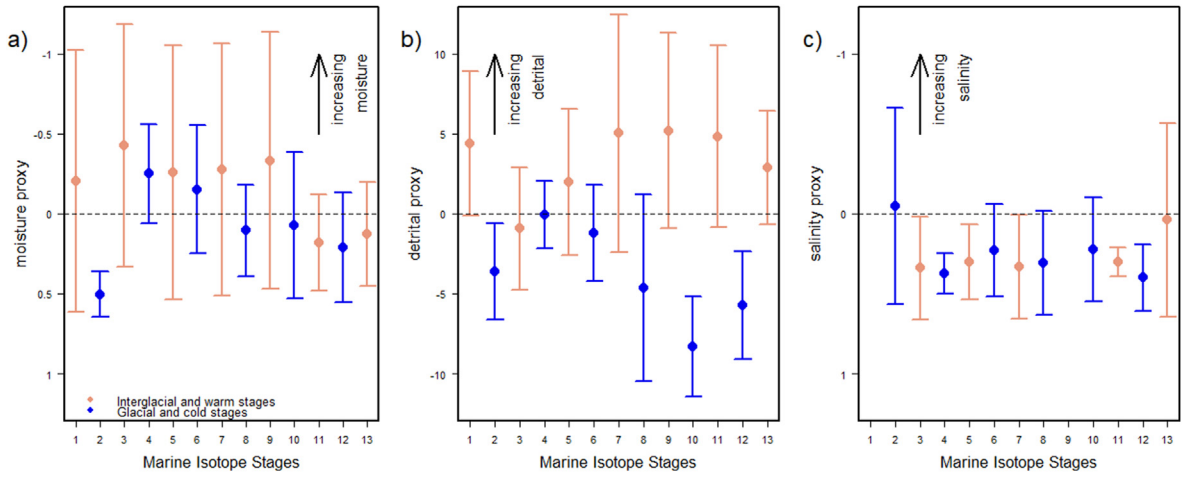

Fig. 9. The mean and standard deviation of SGR proxies moisture (a), detrital (b) and salinity (c) are illustrated across for glacial and interglacial stages for the past 500 kyr.

authigenic uranium being present in sediments of Lake Chalco. The power spectrum of moisture proxy as a function of frequency displays significant peaks corresponding to Earth's major orbital cycles. However, filtering the moisture proxy time series at a 20 kyr frequency band suggests that precession has a dominant effect on moisture (Fig. 8i and j). Overall, average moisture content increased from stage MIS13 to MIS9 (~520–337 ka; Fig. 9a). Lake Chalco likely formed prior or within MIS13, and the lake level rose gradually over time until the interglacial period MIS9 (Fig. 9a). Sediment logical observation such as alternation of fluvial and lacustrine deposits at the MexiDrill site (240–309 m core depth) suggests that the onset of lacustrine deposits occurred between 364 and 505 ka (Valero-Garcés et al., 2021). Moisture levels are higher during interglacials (mean = −0.17) than glacials (mean = 0.08) and interglacial periods had higher variation (mean of standard deviation (σ) for interglacial = 0.66, mean of σ glacial = 0.32). While glacial and cooler periods were drier, two periods, MIS6 and MIS4, still had mean negative moisture proxy values, indicating the presence of authigenic uranium and mostly moist conditions. The driest period, MIS2, was the youngest glacial period.

Variation in our detrital proxy is similar to globally distributed marine benthic oxygen isotopes (LR04 stack; Lisiecki and Raymo, 2005). The power spectrum of the detrital proxy displays significant peaks corresponding with major Earth's orbital cycles (Fig. 8e). Our detrital proxy exhibits a dominant frequency component with ~100 kyr cycles; however, higher frequency components with ~20 kyr cycles are dominating since MIS6 until present. Higher values of our detrital proxy coincide with higher detrital input into Lake Chalco (Fig. 9b). Detrital proxy values are significantly higher during the interglacial (mean = 3.35) than glacial periods (mean = −3.93) indicating higher detrital input to the Lake Chalco during interglacial periods.

The salinity proxy ranging between −1 and +1 with more negative values indicating a higher concentration of cations such as K^+ and likely a shallow lake. Less significant differences between the negative and positive values of the rolling correlation between K and MS indicates that the salinity proxy has low predictability. The power spectrum corresponding to the salinity proxy shows a dominant precession component, but it needs to be considered that this proxy is not available for the full record. The salinity proxy for MIS1 and MIS9 cannot be calculated due to the lack of MS data. Our salinity proxy shows only two stages with higher likelihoods of shallow saline lake conditions, but should be used cautiously (Fig. 9c). The first stage is the interglacial MIS13, the period when the Lake Chalco likely formed. The second is the MIS2 period. However, the diatom record suggests low lake salinity with low evaporation during this period (e.g., Caballero et al., 2019).

4.5. Drivers of moisture

Carbon dioxide, eccentricity, and precession were all key drivers of the moisture content of Lake Chalco over the past 500 kyr. Four models explaining variation in the moisture content have a $\Delta AIC_c <$ 2, indicating they are the top fitting models (Table 1). All models contain the effects of carbon dioxide, eccentricity, and precession, while some top models additionally contain effects of values of a globally distributed marine benthic oxygen isotope ($\delta^{18}O$, an indicator of variation in global ice volume) and obliquity. CO_2 has a positive effect in the moisture content of Lake Chalco in all models (negative values of moisture proxy indicate higher moisture). Eccentricity and precession always have negative effects on lake moisture. Precession oscillation, by changing the direction of tilt of the Earth's axis, controlled the summer and winter insolation in central Mexico. Obliquity and $\delta^{18}O$ have weaker effects on moisture content, probably due to the distance to poles where obliquity acts strongest. However, when present in models, obliquity has a negative effect on moisture, while higher values of $\delta^{18}O$, indicating lower sea surfaces temperatures, has a negative effect on lake moisture.

5. Discussion

5.1. Origin of γ-ray signal

γ-ray radiation among the lacustrine deposits of Lake Chalco primarily varies in response to sediment composition. The main source of radiogenic elements (K, Th, and U) are driven by environmental factors controlling the chemistry of sediments. Weathering of volcanogenic rocks and erosion rates drive temporal variation of radiogenic elements across lacustrine sediments of central Mexico. The rate of weathering is dependent on the exposure of volcanogenic rocks to weathering elements and climate conditions prevailing in central Mexico at a given time (e.g., rate of precipitation). Strong covariance between γ-ray and radiogenic elements with MS (Fig. 1) suggests that the sediments transported from altered volcanogenic rocks are the main source of γ-ray radiation among the lacustrine sediments. The unimodal distribution of the γ-ray signal and positive covariation among the radiogenic

Table 1
AIC_c statistics for models for potential drivers of moisture. $\delta^{18}O$ = stack of globally distributed marine benthic oxygen isotope data (LR04 stack; Lisiecki and Raymo, 2005), E = eccentricity, O = obliquity, P = precession, AIC_c = AIC corrected for small sample size, logLik = log likelihood, *df* = degrees of freedom, R^2 = adjusted regression coefficient, *P* = model *P*-value, delta = difference between the top model and given model AIC_c, w_i = model weight. Only models with $\Delta AIC_c < 2$ are shown for each variable comparison.

Model	Int	CO_2	$\delta^{18}O$	E	O	P	df	logLik	AIC_C	delta	*wi*	R^2	*P*
Model 1	−0.37	0.0017		−0.089	−0.037	−0.049	6	−291.03	594.2	0	0.305	0.062	<0.001
Model 2	−1.04	0.0030	0.093	−0.080	−0.031	−0.053	7	−290.45	595.1	0.91	0.194	0.064	<0.001
Model 3	−1.31	0.0034	0.132	−0.076		−0.054	6	−291.72	595.6	1.38	0.153	0.059	<0.001
Model 4	−0.36	0.0016		−0.088		−0.049	5	−292.98	596.1	1.86	0.12	0.055	<0.001

elements and MS indicate that the distribution of radiogenic elements is a function of a dominant sedimentation mechanism, with higher γ-ray values indicating higher detrital input. To a lesser degree, the existence of both right skewed and unimodal distributions of γ-ray signals (Supplement Material 08) suggests effects of other environmental factors in addition to a detrital origin of the γ-ray signal. For instance, high lake levels can be inferred from high γ radiation, which coincides with excessive U, combined with negative correlations between U and two other radiogenic elements (K and Th). These conditions suggest increased concentrations of authigenic U in response to the development of anoxic redox conditions in bottom water sediments, which are expected to increase with rising lake levels. Enhanced salinity in the lake system is another factor that contributes to the rise of γ radiation by concentrating cations such as K, Th, and U. However, our salinity proxy, although with low predictability, suggests that Lake Chalco has likely experienced evaporation during the interglacial MIS13.

5.2. Astronomical age model and uncertainties

The age model for lacustrine deposits of Lake Chalco has evolved from linking quasi-cyclic variations in the γ-ray stratigraphic record to astronomical references. The astronomical age model is further improved by tuning it with the LR04 stack reference dataset (Lisiecki and Raymo, 2005). The tuned age and duration derived from the cyclostratigraphic analysis supports results from a Bayesian age-depth model of radio-isotopic dating for the upper 130 kyr of the sequence (Martínez-Abarca et al., 2021). Our tuned astronomical age-depth model is suggesting an age of ~500 ka for the entire lacustrine deposits of the Lake Chalco, which is slightly older than the 408 ± 47 ka of the Bayesian age-depth model suggested by Martínez-Abarca et al. (2021). This difference may either occur due to the uncertainties associated with our tuned astronomical age-depth model, or more likely the lack of radiometric dating below 170 m in the Bayesian age-depth model. Uncertainties regarding the astronomical tuned age mainly exist due to three factors: imprecision of tie points, intrinsic uncertainty in the LR04 stack, and delays in the feedbacks of geological responses to glacial-interglacial cycles.

The depth variation around the tie points ranges from 10 cm to 20 cm, but depth inaccuracy can reach 50 cm between tie points. We estimate the maximum uncertainty in depth correlations of the tie points to be in order of 1000 to maximum 10,000 years. An additional potential source of error in our astronomical age model is the inherent uncertainty in the LR04 stack. The LR04 stack is an age model (present to 5.3 Ma) using alternate models of $\delta^{18}O$ records in response to variation in ice volume during Pliocene-Pleistocene period (Lisiecki and Raymo, 2005). The age uncertainty in the LR04 stack is estimated to be less than 4 ka from 1 to 0 Ma, and we adopt this uncertainty measure.

The observed cyclic pattern within the γ-ray time series of Lake Chalco is assumed synchronous with alternating series of glacial and interglacial periods during the Quaternary. Response times of the climate and other Earth system components such as lake and sea surface temperature to glacial and interglacial periods vary (e.g., Meyers, 2017). The interaction of ice volume and atmospheric temperature and the feedback of Lake Chalco to these changes would produce age model errors of at least several thousand years. However, the tuning of our model to the LR04 stack could reduce the duration of this uncertainty type. We estimated that the assumed uncertainties on the constructed ~500 ka astronomical age for lacustrine deposits of Lake Chalco do not exceed 10 ka at/around the tie points. However, the uncertainty may increase up to 20 ka with increasing distance from the tie points.

5.3. Moisture variation across glacial and interglacial periods

After removing the influence of tephra, the three signals representing detrital, salinity, and moisture proxies are derived from the SGR and MS datasets. Together, these proxies reconstruct the evolution of moisture availability across the glacial and interglacial stages of the last ~500 kyr. Although, salinity proxy has less predictive power compared to detrital and moisture proxies. In this section, we discuss the evolution of our SGR proxies over time in respect to the available sedimentological, geochemical, paleontological, and rock magnetic data sets reported on the lacustrine deposits of Lake Chalco.

Our moisture proxy indicates a shallow and oxygenated aquatic system during the transition period from an alluvial-fluvial to lacustrine system (MIS13 - MIS12, or ~520–470 ka). The likelihood of authigenic uranium development was low due to a lack of reducing conditions in bottom waters during MIS13 to MIS12. Absence of aquatic organisms and geochemical evidence for denitrification in the sediments deposited prior to the onset of Lake Chalco suggest a shallow and unproductive (oligotrophic) aquatic system (Martínez-Abarca et al., 2021), consistent with our moisture proxy recorded during the MIS13 and MIS12. Similar conditions of an oxygen-rich freshwater body have been proposed for Lake Tequixquiac in the northern Basin of Mexico during MIS13 and MIS12 (Toole, 2019). Lake Tequixquiac was located 60 km north of Lake Chalco in the northernmost part of the Basin of Mexico. Our salinity proxy indicates the existence of possibly marshy highly saline environments during MIS13, derived from the clear increase in K content relative to MS. High salinity levels at a transition period from alluvial-fluvial stage to lacustrine stage is evinced through the carbon and nitrogen isotope signatures ($\delta^{13}C < -28‰$, $\delta^{15}N \sim 5.5‰$; Martínez-Abarca et al., 2021) of Lake Chalco's sediments. Simultaneous, shallow ephemeral aquatic systems containing several saltwater pools in Lake Tequixquiac have been linked to warm and arid conditions possibly due to strong El Niño-like climate cycles (Toole, 2019).

Our moisture proxy suggests lake levels remained low during the MIS11 (424–374 ka) and MIS10 (374–337 ka). However, water levels increased gradually towards creating a large water body (MIS10). Rises in diatom and aquatic organisms (e.g. bivalves) suggest an evolution to a deeper eutrophic lake (Martínez-Abarca et al., 2021; Valero-Garcés et al., 2021). The moisture proxy demonstrates a higher lake level in MIS10 than during previous MIS

(MIS13 – MIS11). This is in line with the idea of extension of Lake Chalco during MIS10 due to the occurrence of first lacustrine carbonate and abundant algal biomass ($\delta^{15}N \gg 6.8‰$; Martínez-Abarca et al., 2021). Our detrital proxy indicates higher runoff to the Chalco basin during the interglacial stages compared to the glacial stages prior to the MIS10. However, higher runoff was not able to increase water depth to levels required for developing anoxic conditions in bottom sediments, likely due to increasing expansion of the lake area.

The moisture content rose rapidly from glacial stage MIS10 to interglacial stage MIS9, which is indicating an abrupt climate change. A gradual rise of available moisture recorded throughout the passage from MIS9 (~337 ka) up to the interstadial stage of MIS3 (~30 ka). Our moisture proxy indicates higher variation during warmer periods including interglacial stages. In contrast, moisture availability exhibited lower variation during glacial and cooler stages (Fig. 9a). However, overall moisture increased from MIS9 to MIS3. Variation in moisture content across cold/warm stages are reflected in physical, chemical and biological characteristic of lacustrine deposits of the Lake Chalco. For example, our moisture proxy suggests Lake Chalco experienced higher moisture content during the MIS4 and MIS6 compared to the other glacial and cold stages, in agreement with previous paleontological results from Lake Chalco (Fig. 6, Ortega-Guerrero et al., 2020).

The higher variation in the moisture proxy values during interglacial stages indicates the existence of a long-term alternation between wet and dry periods that were likely controlled by the position of the ITCZ in response to the seasonal variation (e.g., Lozano-García et al., 2015; Metcalfe et al., 2015). For instance, highest amplitude variability of magnetic parameters occurred during MIS5 (Ortega-Guerrero et al., 2020), and we see the same for the SGR. Another example for a higher variability in moisture during the interglacial are the dominant drought conditions at the end of MIS5 (~85 ka; Torres-Rodríguez et al., 2015) which shortly switch to wetter conditions, evinced by an increasing abundance of freshwater diatoms c. 80 ka (Ortega-Guerrero et al., 2020). The last and penultimate glacial wet periods were longer than the dry periods, causing a remarkable rise in moisture content during the glacial stages of MIS6 (191–130 ka) and the cooler stage of MIS4 (71–57 ka). For instance, clear increases in diatom species such as *Stephanodiscus niagarae* in the lacustrine deposits of Lake Chalco indicate the presence of a deep lake phase during MIS6 (Avendaño-Villeda et al., 2018).

Following the gradual increases in moisture from MIS9 to MIS3, our detrital proxy exhibits a gradual decreasing trend, indicating higher precipitation but lower surface runoff due to higher vegetation on land and hence lower sediment availability. This is in line with paleontological evidence indicating the dominance of pine forests prior or within MIS3 (e.g., Lozano-García and Ortega-Guerrero, 1998).

Our results suggest that Lake Chalco experienced the lowest lake levels during the glacial stage of MIS2 (29–14 ka). Lower detrital proxy values indicate low surface runoff and groundwater in surrounding highlands during MIS2. The paleontological and sedimentological evidence combined with our SGR proxies confirm an abrupt climate change toward an extreme dry conditions in central Mexico during a transition from interglacial stage of MIS3 to glacial stage of MIS2 (~31–28 ka; e.g., Lozano-García et al., 2015; Caballero et al., 2019). This may correspond to the worldwide dry phase during the Last Glacial Maximum (LGM; 29–16 ka, e.g., Hughes, 2021).

Development of an extensive glacial phase on top of volcanic chains around the Basin of Mexico between ~21 ka and 17.5 ka lowered the glacier equilibrium line to 3940 m a.s.l. (almost 1000 m lower than the crest of volcanoes), and reduced the mean annual temperature by 6–8 °C (e.g., Vazquez-Selem and Heine, 2011). Dry and cold conditions during MIS2 are reflected in reduced runoff and low lacustrine productivity at Lake Chalco (Lozano-García et al., 2015). This is consistent with our moisture and detrital proxies recorded during the MIS2. Expansion of juniper forests around Lake Chalco between 27 and 26.5 ka additionally suggests dominance of dry conditions in the Basin of Mexico (Lozano-García and Ortega-Guerrero, 1994, 1998).

Paleontological and geochemical studies suggest that dry conditions occurred long before the onset of the LGM in central Mexico, during the transition from MIS3 to MIS2 (c. 38–29 ka, Caballero and Ortega-Guerrero, 1998; Roy et al., 2009). Drought conditions eventually led to the disconnection of Lake Chalco from other lakes in central Mexico (Caballero and Ortega-Guerrero, 1998; Cantarero, 2013). Lake Chalco's separation from other lakes in central Mexico is clearly reflected in our moisture proxy signal around 37 ka, where a clear drop in moisture occurs (Fig. 8i). Our moisture proxy displays a declining trend in moisture toward MIS1 since the closure of Lake Chalco.

5.4. Astronomical forcing of lacustrine sedimentation

Our detrital proxy exhibits clear similarity with the LR04 benthic stack (Lisiecki and Raymo, 2005) in all orbital cycles over the last ~500 kyr (Fig. 8). The strong ~100 kyr cycles imply that glacial – interglacial cycles were the primary factor in controlling the variation of detrital content to Lake Chalco prior to the glacial stage of MIS6. Our detrital proxy exhibits higher frequency components from MIS6 until present (Fig. 8e), which is mainly associated with climatic precession. This higher frequency component has already been reported in many proxy records within the last 150 kyr in lacustrine deposits of Lake Chalco (e.g., Lozano-García et al., 2015; Caballero et al., 2019; Ortega-Guerrero et al., 2020; Martínez-Abarca et al., 2021). The salinity proxy and its power spectrum (Fig. 8g and h) reveals a weak evidence of precession cycles with a period of about 20 kyr, although the pattern is incomplete.

The moisture proxy exhibits strong and dominating precession components with a period of ~20 kyr in all parts of the record (Fig. 8i and j). This indicates the role of precession-derived insolation in precipitation in central Mexico. Eccentricity and obliquity are other factors controlling the moisture content indicating the effect of glacial – interglacial cycles on precipitation in central Mexico within the last 500 kyr.

The positive effect of CO_2 on our moisture proxy suggests glacial-interglacial cycles drove precipitation in central Mexico (Table 1). Generally, temperature increases with CO_2 - indicating an interglacial stage, which coincides with higher moisture content in the case of Lake Chalco. This is in agreement with increasing detrital input due to higher runoff to Lake Chalco during the interglacial stages relative to glacial stages. A positive effect of eccentricity on available moisture content aligns with the relationship between glacial-interglacial cycles and precipitation rate within the 100 kyr cycle. Earth receives minimum amounts of solar radiation when its orbit is most circular, triggering glacial periods and generally dry conditions. The effect of precession on our moisture proxy points the effect of precession-derived insolation on tropical precipitation. Earth's precession controls variation in seasonal solar radiation by changing the thermal gradient between the two hemispheres. Further, intense solar radiation warms ocean waters and causes an area with high humidity. The westward trade winds transfer the moisture out of the tropical Atlantic Ocean across Central America and rains out into the Pacific Ocean. Our results suggest that the interplay between northward and southward shifts of the ITCZ, forced by both precession and glacial/

interglacial climate states are most likely the cause of precipitation patterns in central Mexico on a ~20 kyr orbital scales.

6. Conclusions

Using spectral γ-ray borehole logging data, we establish an astronomical age-depth model refined by correlation to a marine oxygen isotope stack. γ-ray has mostly a detrital origin when disregarding ash layers. We detect regular quasi-cyclic patterns in γ-ray logs across the upper 300 m deposits of Lake Chalco with dominant periods of 50 m, 23 m, 10 m, and 5 m. An average SR of 43.5 cm/kyr is estimated using timeOpt analysis with strong concentration of spectral power at 100 and 19 kyr cycles. Our cyclostratigraphic timeframe for lacustrine deposits of Lake Chalco is comparable with the Pleistocene benthic stack. This astronomical tuned timeframe was calibrated additionally with previously obtained radiogenic ages, allowing us to estimate the duration of lacustrine deposits of Lake Chalco slightly over a period of 500 kyr with an uncertainty ranging from 5 to 20 kyr.

Further, we reconstruct detrital input, salinity and moisture availability for Lake Chalco over the last 500 kyr. We find that the contribution of radioactive elements (K, Th, and U) among lacustrine sediments of Lake Chalco vary with climatic and environmental conditions over time. Increasing runoff to the basin elevated the concentration of radiogenic elements and magnified γ radiation among lacustrine sediments. Detrital input dropped during the glacial droughts and significantly rose during the interglacial wet periods in a 100 kyr cycles. During interglacial stages, higher precipitation contributed to the rising lake level at Lake Chalco and resulted in concentration of authigenic uranium in bottom sediments, in turn boosting γ radiation. Moisture variability in central Mexico occurred in a cyclic pattern with ~20 kyr cycles.

Through controlling atmospheric CO2, our model suggests that Earth's orbital eccentricity and precession determined long-term moisture availability for the last 500 kyr in central Mexico. Lake Chalco routinely underwent a dry period when Earth's orbit was in its most circular shape throughout the last 500 ka. Within the glacial and cold stages, Lake Chalco experienced two relatively wet periods in the time of MIS6 (191–130 ka) and MIS4 (71–57 ka), and extreme dry condition through the MIS2 (29–14 ka). We found that precession derived-insolation by controlling the position of the ITCZ is likely the cause of 20 kyr cycles in central Mexico. In sum, we show that downhole logging measurements can be a key tool to unravel the climate record of the Quaternary.

Author statement

TW led the Lake Chalco project and supported the scientific discussion on downhole logging data acquisition and interpretation. CZ and AU contributed the scientific discussion of cyclostratigraphy. MSA analyzed the data and wrote the first draft. All authors contributed to writing the final manuscript.

Declaration of competing interest

The authors declare that they have no known competing financial interests or personal relationships that could have appeared to influence the work reported in this paper.

Data availability

Data will be made available on request.

Acknowledgments

The International Continental Scientific Drilling Program, US National Science Foundation and Universidad Nacional Autónoma de México have funded the MexiDrill Field campaign. The Leibniz Institute for Applied Geophysics (LIAG) supported this research. We sincerely appreciate the contribution of Thomas Grelle, Carlos Lehne, and Jan-Thorsten Blake in acquisition of the downhole logging measurements. We greatly acknowledge the MexiDrill team for their scientific and logistic support. We thank P. Rioual, and two anonymous reviewers for constructive reviews.

Appendix A. Supplementary data

Supplementary data to this article can be found online at https://doi.org/10.1016/j.quascirev.2022.107739.

References

Amador, J.A., Alfaro, E.J., Lizano, O.G., Magaña, V.O., 2006. Atmospheric forcing of the eastern tropical Pacific: a review. Prog. Oceanogr. 69 (2), 101–142. https://doi.org/10.1016/j.pocean.2006.03.007.

Arce, J.L., Layer, P.W., Lassiter, J.C., Benowitz, J.A., Macías, J.L., Ramírez-Espinosa, J., 2013. $^{40}Ar/^{39}Ar$ dating, geochemistry, and isotopic analyses of the quaternary Chichinautzin volcanic field, south of Mexico City: implications for timing, eruption rate, and distribution of volcanism. Bull. Volcanol. 75 (12), 1–25. https://doi.org/10.1007/s00445-013-0774-6.

Arce, J.L., Layer, P.W., Macías, J.L., Morales-Casique, E., García-Palomo, A., Jiménez-Domínguez, F.J., Benowitz, J., Vásquez-Serrano, A., 2019. Geology and stratigraphy of the Mexico basin (Mexico City), central trans-Mexican volcanic belt. J. Maps 15 (2), 320–332. https://doi.org/10.1080/17445647.2019.1593251.

Avendaño-Villeda, D.A., Caballero, M., Ortega-Guerrero, B., Lozano-García, S., Brown, E., 2018. Condiciones ambientales a finales del Estadio Isotópico 6 (EI 6: > 130000 años) en el centro de México: caracterización de una sección de sedimentos laminados proveniente del Lago de Chalco. Rev. Mex. Ciencias Geol. 35 (2), 168–178.

Bárton, K., 2020. MuMIn: Model Selection and Model Averaging Based on Information Criteria (AICc and Alike). R package version 1.43.17.

Baumgarten, H., Wonik, T., 2015. Cyclostratigraphic studies of sediments from Lake Van (Turkey) based on their uranium contents obtained from downhole logging and paleoclimatic implications. Int. J. Earth Sci. 104 (6), 1639–1654. https://doi.org/10.1007/s00531-014-1082-x.

Brown, E.T., Caballero, M., Cabral Cano, E., Fawcett, P.J., Lozano-García, S., Ortega, B., Pérez, L., Schwalb, A., Smith, V., Steinman, B.A., Stockhecke, M., Valero-Garcés, B., Watt, S., Wattrus, N.J., Werne, J.P., Wonik, T., Myrbo, A.E., Noren, A.J., O'Grady, R., Schnurrenberger, D., 2019. Scientific drilling of lake Chalco, Basin of Mexico (MexiDrill). Sci. Drill. 26, 1–15. https://doi.org/10.5194/sd-26-1-2019 the MexiDrill Team.

Burnham, K.P., Anderson, D.R., 2003. Model Selection and Multimodel Inference: a Practical Information-Theoretic Approach. Springer Science & Business Media, New York, USA. https://doi.org/10.1007/b97636.

Caballero, M., Ortega-Guerrero, B., 1998. lake levels since about 40,000 years ago at Lake Chalco, near Mexico city. Quat. Res. 50 (1), 69–79. https://doi.org/10.1006/qres.1998.1969.

Caballero, M., Lozano-García, S., Ortega-Guerrero, B., Correa-Metrio, A., 2019. Quantitative estimates of orbital and millennial scale climatic variability in Central Mexico during the last ~40,000 years. Quat. Sci. Rev. 205, 62–75. https://doi.org/10.1016/j.quascirev.2018.12.002.

Cantarero, S., 2013. Multiproxy Paleoclimatic Record from Geochemical Analyses of Lake Chalco Sediments, a Closed Basin Lake in Central Mexico. Master dissertation, University of Minnesota, p. 96.

Chalk, T.B., Hain, M.P., Foster, G.L., Rohling, E.J., Sexton, P.F., Badger, M.P., Cherry, S.G., Hasenfratz, A.P., Haug, G.H., Jaccard, S.L., Martínez-García, A., 2017. Causes of ice age intensification across the Mid-Pleistocene Transition. Proc. Natl. Acad. Sci. USA 114 (50), 13114–13119. https://doi: 10.1073/pnas.1702143114.

Dräger, N., Plessen, B., Kienel, U., Słowiński, M., Ramisch, A., Tjallingii, R., Pinkerneil, S., Brauer, A., 2019. Hypolimnetic oxygen conditions influence varve preservation and $\delta^{13}C$ of sediment organic matter in Lake Tiefer See, NE Germany. J. Paleolimnol. 62 (2), 181–194. https://doi.org/10.1007/s10933-019-00084-2.

Ferrari, L., Orozco-Esquivel, T., Manea, V., Manea, M., 2012. The dynamic history of the Trans-Mexican Volcanic Belt and the Mexico subduction zone. Tectonophysics 522, 122–149. https://doi.org/10.1016/j.tecto.2011.09.018.

Gouhier, T.C., Grinsted, A., Simko, V., 2021. R Package Biwavelet: Conduct Univariate and Bivariate Wavelet Analyses. Version 0.20. 21.

Hamnett, B.R., 2006. A Concise History of Mexico. Cambridge University Press, p. 538.

Hendriks, P.H.G.M., Limburg, J., De Meijer, R.J., 2001. Full-spectrum analysis of natural γ-ray spectra. J. Environ. Radioact. 53 (3), 365–380. https://doi.org/10.1016/S0265-931X(00)00142-9.
Herrera-Hernández, D., 2011. Estratigrafía y análsisi de facies de los sedimentos lacustres del Cuaternario tardío de la cuenca de Chalco, México. Master thesis. Instituto de Geofísica Universidad Nacional Autónoma de México, p. 122.
Hughes, P.D., 2021. Concept and global context of the glacial landforms from the Last Glacial Maximum. In: Palacios, D., Hughes, P.D., Ruiz, J.M.G., Andrés, N.D. (Eds.), European Glacial Landscapes: Maximum Extent of Glaciations. Elsevier, Amsterdam, pp. 355–358. https://doi.org/10.1016/B978-0-12-823498-3.00039-X.
James, G., Witten, D., Hastie, T., Tibshirani, R., 2017. An Introduction to Statistical Learning, eighth ed. Springer Science+Business Media, New York, p. 426.
Kirkwood, J.B., 2010. The History of Mexico, second ed. Greenwood Press, An Imprint of ABC–CLIO, LLC, Santa Barbara, CA, p. 258.
Laskar, J., Robutel, P., Joutel, F., Gastineau, M., Correia, A.C.M., Levrard, B., 2004. A long-term numerical solution for the insolation quantities of the Earth. Astron. Astrophys. 428 (1), 261–285. https://doi.org/10.1051/0004-6361:20041335.
Li, M., Huang, C., Ogg, J., Zhang, Y., Hinnov, L., Wu, H., Chen, Z.Q., Zou, Z., 2019. Paleoclimate proxies for cyclostratigraphy: comparative analysis using a Lower Triassic marine section in South China. Earth Sci. Rev. 198, 125–146. https://doi.org/10.1016/j.earscirev.2019.01.011.
Lisiecki, L.E., Raymo, M.E., 2005. A Pliocene-Pleistocene stack of 57 globally distributed benthic $\delta^{18}O$ records. Paleoceanography 20, PA1003. https://doi:10.1029/2004PA001071.
Lüthi, D., Le Floch, M., Bereiter, B., Blunier, T., Barnola, J.M., Siegenthaler, U., Raynaud, D., Jouzel, J., Fischer, H., Kawamura, K., Stocker, T.F., 2008. High-resolution carbon dioxide concentration record 650,000–800,000 years before present. Nature 453 (7193), 379–382. https://doi.org/10.1038/nature06949.
Lozano-García, M.S., Ortega-Guerrero, B., 1994. Palynological and magnetic susceptibility records of Lake Chalco, central Mexico. Palaeogeogr. Palaeoclimatol. Palaeoecol. 109, 177–191. https://doi.org/10.1016/0031-0182(94)90175-9.
Lozano-García, M.S., Ortega-Guerrero, B., 1998. Late Quaternary environmental changes of the central part of the Basin of Mexico: correlation between Texcoco and Chalco basins. Rev. Palaeobot. Palynol. 99, 77–93. https://doi.org/10.1016/S0034-6667(97)00046-8.
Lozano-García, S., Ortega, B., Roy, P.D., Beramendi-Orosco, L., Caballero, M., 2015. Climatic variability in the northern part of the American tropics since the latest MIS 3. Quat. Res. 85 (2), 261–272. https://doi.org/10.1016/j.yqres.2015.07.002.
Martínez-Abarca, L.R., Lozano-García, S., Ortega-Guerrero, B., Chávez-Lara, C.M., Torres-Rodríguez, E., Caballero, M., Brown, E.T., Sosa-Nájera, S., Acosta-Noriega, C., Sandoval-Ibarra, V., 2021. Environmental changes during MIS6-3 in the Basin of Mexico: a record of fire, lake productivity history and vegetation. J. S. Am. Earth Sci. 109. https://doi.org/10.1016/j.jsames.2021.103231, 103231.
Mazari-Hiriart, M., Tapia-Palacios, M.A., Zarco-Arista, A.E., Espinosa-García, A.C., 2019. Challenges and opportunities on urban water quality in Mexico City. Front. Environ. Sci. 7, 169. https://doi.org/10.3389/fenvs.2019.00169.
Metcalfe, S.E., Barron, J.A., Davies, S.J., 2015. The Holocene history of the North American Monsoon: 'known knowns' and 'known unknowns' in understanding its spatial and temporal complexity. Quat. Sci. Rev. 120, 1–27. https://doi.org/10.1016/j.quascirev.2015.04.004.
Metcalfe, S.E., Nash, D.J., 2012. Quaternary Environmental Change in the Tropics. Wiley-Blackwell, New Jersey, p. 440.
Metcalfe, S.E., O'Hara, S.L., Caballero, M., Davies, S.J., 2000. Records of Late Pleistocene-Holocene climatic change in Mexico - a review. Quat. Sci. Rev. 19 (7), 699–721. https://doi.org/10.1016/S0277-3791(99)00022-0.
Meyers, S.R., 2014. Astrochron: an R Package for Astrochronology.
Meyers, S.R., 2015. The evaluation of eccentricity-related amplitude modulation and bundling in paleoclimate data: an inverse approach for astrochronologic testing and time scale optimization. Paleoceanography 30 (12), 1625–1640. https://doi.org/10.1002/2015PA002850.
Meyers, S.R., 2019. Cyclostratigraphy and the problem of astrochronologic testing. Earth Sci. Rev. 190, 190–223. https://doi.org/10.1016/j.earscirev.2018.11.015.
Meyers, S.R., 2017. Cracking the palaeoclimate code. Nature 546, 219–220. https://doi.org/10.1038/nature22501.
Och, L.M., Müller, B., März, C., Wichser, A., Vologina, E.G., Sturm, M., 2016. Elevated uranium concentrations in Lake Baikal sediments: burial and early diagenesis. Chem. Geol. 441, 92–105. https://doi.org/10.1016/j.chemgeo.2016.08.001.
Ortega-Guerrero, B., Lozano-García, S., Herrera-Hernández, D., Caballero, M., Beramendi-Orosco, L., Bernal, J.P., Torres-Rodríguez, E., Avendaño-Villeda, D., 2017. Lithostratigraphy and physical properties of lacustrine sediments of the last ca. 150 kyr from Chalco basin, central México. J. S. Am. Earth Sci. 79, 507–524. https://doi.org/10.1016/j.jsames.2017.09.003.
Ortega-Guerrero, B., Avendaño, D., Caballero, M., Lozano-García, S., Brown, E.T., Rodríguez, A., García, B., Barceinas, H., Soler, A.M., Albarrán, A., 2020. Climatic control on magnetic mineralogy during the late MIS 6-Early MIS 3 in Lake Chalco, central Mexico. Quat. Sci. Rev. 230, 106–163. https://doi.org/10.1016/j.quascirev.2020.106163.
Peterson, L.C., Haug, G.H., Hughen, K.A., Rohl, U., 2000. Rapid changes in the hydrologic cycle of the tropical Atlantic during the last glacial. Science 290 (5498), 1947–1951. https://doi.org/10.1126/science.290.5498.1947.
R Core Team, 2022. R: A Language and Environment for Statistical Computing. R Foundation for Statistical Computing, Vienna, Austria. http://www.R-project.org.
Read, J.F., Li, M., Hinnov, L.A., Nelson, C.S., Hood, S., 2020. Testing for astronomical forcing of cycles and gamma ray signals in outer shelf/upper slope, mixed siliciclastic-carbonates: upper Oligocene, New Zealand. Palaeogeogr. Palaeoclimatol. Palaeoecol. 555, 109821. https://doi.org/10.1016/j.palaeo.2020.109821.
Roy, P.D., Caballero, M., Lozano, R., Pi, T., Morton, O., 2009. Late pleistocene-holocene geochemical history inferred from Lake tecocomulco sediments, Basin of Mexico, Mexico. Geochem. J. 43 (1), 49–64. https://doi.org/10.2343/geochemj.1.0006.
Snyder, C.W., 2016. Evolution of global temperature over the past two million years. Nature 538 (7624), 226–228. https://doi.org/10.1038/nature19798.
Taner, M.T., 1992. In: Attributes Revisited (Technical Report, Rock Solid Images, Inc) url:
Timofeev, A., Migdisov, A.A., Williams-Jones, A.E., Roback, R., Nelson, A.T., Xu, H., 2018. Uranium transport in acidic brines under reducing conditions. Nat. Commun. 9 (1), 1–7. https://doi.org/10.1038/s41467-018-03564-7.
Thomson, D.J., 1982. Spectrum estimation and harmonic analysis. Proc. IEEE 70, 1055–1096. https://doi.org/10.1109/PROC.1982.12433.
Toole, E., 2019. Palaeoenvironmental and Palaeogeographic Reconstruction of the Tequixquiac Basin, Central Eastern Mexico: Mid to Late Pleistocene Environments. Doctoral Dissertation. Liverpool John Moores University, p. 330.
Torres-Rodríguez, E., Lozano-García, S., Roy, P., Ortega, B., Beramendi-Orosco, L., Correa-Metrio, A., Caballero, M., 2015. Last Glacial droughts and fire regimes in the central Mexican highlands. J. Quat. Sci. 30 (1), 88–99. https://doi.org/10.1002/jqs.2761.
Ulfers, A., Hesse, K., Zeeden, C., Russell, J.M., Vogel, H., Bijaksana, S., Wonik, T., 2021. Cyclostratigraphy and paleoenvironmental inference from downhole logging of sediments in tropical Lake Towuti, Indonesia. J. Paleolimnol. 65 (4), 377–392. https://doi.org/10.1007/s10933-020-00171-9.
Ulfers, A., Zeeden, C., Wagner, B., Krastel, S., Buness, H., Wonik, T., 2022. Borehole logging and seismic data from Lake Ohrid (North Macedonia/Albania) as a basis for age-depth modelling over the last one million years. Quat. Sci. Rev. 276, 107295. https://doi.org/10.1016/j.quascirev.2021.107295.
Valero-Garcés, B., Stockhecke, M., Lozano-García, S., Ortega, B., Caballero, M., Fawcett, P., Werne, J.P., Brown, E., Najera, S.S., Pearthree, K., McGee, D., 2021. Stratigraphy and sedimentology of the upper Pleistocene to holocene Lake Chalco drill cores (Mexico basin). In: Rosen, M.R., Finkelstein, D.B., Park Boush, L., Pla-Pueyo, S. (Eds.), Limnogeology: Progress, Challenges and Opportunities : A Tribute to Elizabeth Gierlowski-Kordesch. Springer International Publishing, Cham, pp. 415–443. https://doi.org/10.1007/978-3-030-66576-0_14.
Vazquez-Selem, L., Heine, K., 2011. Late quaternary glaciation in Mexico. In: Ehlers, J., Gibbard, P.L. (Eds.), Quaternary Glaciations - Extent and Chronology, Part III: South America, Asia, Africa, Australia, Antarctica. Elsevier, Amsterdam, pp. 233–242.
Welti, E.A., Roeder, K.A., de Beurs, K.M., Joern, A., Kaspari, M., 2020. Nutrient dilution and climate cycles underlie declines in a dominant insect herbivore. Proc. Natl. Acad. Sci. USA 117 (13), 7271–7275. https://doi.org/10.1073/pnas.1920012117.
Willeit, M., Ganopolski, A., Calov, R., Brovkin, V., 2019. Mid-Pleistocene transition in glacial cycles explained by declining CO2 and regolith removal. Sci. Adv. 5 (4), eaav7337. https://doi.org/10.1126/sciadv.aav7337.
Zeeden, C., Meyers, S.R., Lourens, L.J., Hilgen, F.J., 2015. Testing astronomically tuned age models. Paleoceanography 30 (4), 369–383. https://doi.org/10.1002/2014PA002762.